Clays and Clay Minerals, Vol. 36, No. 1, 1–10, 1988.

MICROSTRUCTURES, FORMATION MECHANISMS, AND DEPTH-ZONING OF PHYLLOSILICATES IN GEOTHERMALLY ALTERED SHALES, SALTON SEA, CALIFORNIA[1]

YU-CHYI YAU,[2] DONALD R. PEACOR,[2] RICHARD E. BEANE,[2,4]
ERIC J. ESSENE,[2]

[2] Department of Geological Sciences, University of Michigan
Ann Arbor, Michigan 48109

AND S. DOUGLAS MCDOWELL[3]

[3] Department of Geology and Geological Engineering
Michigan Technological University
Houghton, Michigan 49931

Abstract—Scanning, transmission, and analytical electron microscopy studies of shales from the Salton Sea geothermal field revealed that phyllosilicates progress through zones of illite-muscovite (115°–220°C), chlorite (220°–310°C), and biotite (310°C). These phyllosilicates occur principally as discrete, euhedral to subhedral crystals which partly fill pore space. The structural and chemical heterogeneity, which is typical of phyllosilicates in shales subject to diagenesis, is generally absent. Textures and microstructures indicate that the mineral progression involves dissolution of detrital phases, mass transport through interconnecting pore space, and direct crystallization of phyllosilicates from solution.

Phyllosilicate stability relations indicate that either increase in temperature or changing ion concentrations in solutions with depth are capable of explaining the observed mineral zoning. Textural and compositional data suggest that the observed mineral assemblages and the interstitial fluids approach equilibrium relative to the original detrital suites. The alteration process may have occurred in a single, short-lived, episodic hydrothermal event in which the original detrital phases (smectite, etc.) reacted directly to precipitate illite, chlorite, or biotite at different temperatures (depths) without producing intermediate phases.

Key Words—Chlorite, Electron microscopy, Fluid-mineral equilibria, Geothermal field, Illite, Salton Sea, Smectite, Texture.

INTRODUCTION

Phyllosilicate reactions during low-grade burial metamorphism of argillaceous sediments may result in a characteristic sequence of phyllosilicates as a function of burial depth. A significant reaction involves the progressive change of smectite through interstratified illite/smectite to illite (Weaver, 1959; Burst, 1969; Perry and Hower, 1970; Hower *et al.*, 1976) and the subsequent transition of illite to muscovite (Velde and Hower, 1963; Maxwell and Hower, 1967) as a result of increasing temperature and pressure during burial diagenesis. Concomitantly, chlorite may increase in abundance with depth (Hower *et al.*, 1976). The diagenetic chlorite has been inferred to be a direct by-product of the smectite-to-illite reaction (Ahn and Peacor, 1985), as it is commonly intergrown as packets of layers or as a mixed-layer phase with illite. Both the illite and chlorite formed from precursor smectite through a replacement mechanism (Hower *et al.*, 1976; Ahn and Peacor, 1985, 1986).

On the basis of powder X-ray diffraction (XRD) studies, a generalized smectite-to-illite reaction has been described as taking place in shallow samples from the Salton Sea geothermal field (Muffler and White, 1969; McDowell and Elders, 1980). From a transmission electron microscopy (TEM) study of textures and microstructures of clays in Salton Sea shales, Yau *et al.* (1987a) concluded that most of the illite formed as discrete euhedral crystals by direct precipitation from solution in void space and not as a direct replacement of smectite. The absence of pre-existing smectite and illite/smectite in contact with discrete illite suggests that smectite dissolved in hydrothermal fluids, from which illite subsequently precipitated. Yau *et al.* (1987a) proposed that such a dissolution-precipitation mechanism is compatible with an open system and a relatively high water/rock ratio, whereas the replacement mechanism dominates in relatively closed systems, such as Gulf coast shales. Their results suggest that the chlo-

[1] Contribution No. 433 from the Mineralogical Laboratory, Department of Geological Sciences, University of Michigan, Ann Arbor, Michigan 48109.

[4] Present address: St. Joe American Corporation, 2002 N. Forbes Blvd., Tucson, Arizona 85745.

https://doi.org/10.1346/CCMN.1988.0360101 Published online by Cambridge University Press

rite and biotite in the Salton Sea sediments (McDowell and Elders, 1980) would have formed by a dissolution-precipitation mechanism and that the resulting texture would differ from that observed in most burial metamorphic sequences, such as the Gulf Coast shales (Lee *et al.*, 1985; Ahn and Peacor, 1986).

Phase relations among mineral assemblages and interstitial fluids from the Salton Sea geothermal system were calculated by Helgeson (1967, 1968), Bird and Norton (1981), and Bird *et al.* (1984); however, the phase relations among illite, chlorite, and biotite and their variation with temperature, fluid composition, and solid solution have not yet been completely characterized in the Salton Sea system. The objective of the present study was to investigate formation mechanisms of phyllosilicates in that system and to formulate the equilibrium conditions of their formation and for their changes with depth. Textural and compositional data were used to test whether or not equilibrium or disequilibrium relations adequately describe the sequence of changes in geothermally altered shales.

SAMPLE CHARACTERIZATION AND STUDY METHODS

The Salton Sea geothermal field (SSGF), California, is underlain by deltaic sediments that were deposited beginning in the Pliocene or late Miocene from the Colorado River (Muffler and White, 1969). The original shaly sediments were compositionally similar to the modern deltaic Colorado River muds and consisted predominantly of quartz, plagioclase, K-feldspar, calcite, dolomite, illite/smectite, and kaolinite (Muffler and Doe, 1968). The development of the SSGF is related to recent rhyolitic volcanism that is associated with an active, oceanic basalt-producing, transform-fault system (Robinson *et al.*, 1976).

Samples for the present study were cuttings recovered from well IID No. 2. The upper part of the section consists of about 1000 m of shale containing a few sand stringers (Figure 1; Helgeson, 1968). This shale section becomes more sandy with depth, grading into arkosic sand, which contains some argillaceous intervals, to a depth of 1547 m. The variation of temperature with depth was taken from the data for well IID No. 2 (Helgeson, 1968).

Progressive changes in the texture and chemistry with depth and temperature were described for phyllosilicates in sandstones from the Elmore 1 well from the SSGF (McDowell and Elders, 1980, 1983). The detailed textures and compositions of phyllosilicates in shales were not completely characterized, due to the very fine grained character of the shales; the small particles are beyond the resolution of most conventional analytical techniques, such as electron microprobe analysis. In the present study scanning and transmission electron microscopy (SEM, TEM) and analytical electron microscopy (AEM) were used to investigate the shales.

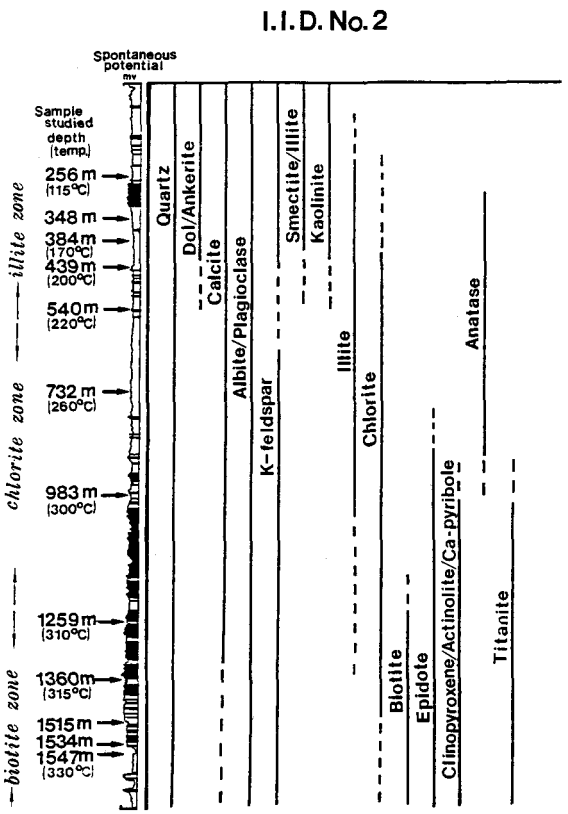

Figure 1. Schematic drawing of lithologic, temperature, and mineral variations with depth. In lithology column, clear = shale; solid = sandstone. Vertical bars show depth range of specific minerals in shales—solid where common, dashed where not common.

Shale cuttings were first analyzed by XRD to provide an overall picture of mineralogical changes with depth. Bulk rock chemistry of shale from selected depths was obtained by X-ray fluorescence (XRF) analysis at the Michigan Technological University. For electron microscopic studies, shale cuttings were impregnated with casting resin and then sectioned along randomly oriented planes for petrographic thin sections. Following optical examination, 3-mm diameter areas of samples were detached from the thin sections and ion-thinned by argon beam bombardment. The ion-thinned samples were then observed using Hitachi scanning and JEOL 100-CX transmission electron microscopes. Semiquantitative compositions of phyllosilicates were obtained from ion-thinned areas (400 × 400 Å) by AEM. Well-analyzed, ion-thinned clinochlore was used as a standard for Mg/Si, adularia for K/Si and Al/Si, and fayalite for Fe/Si. Procedures for AEM analysis of samples were described in detail by Isaacs *et al.* (1981).

https://doi.org/10.1346/CCMN.1988.0360101 Published online by Cambridge University Press

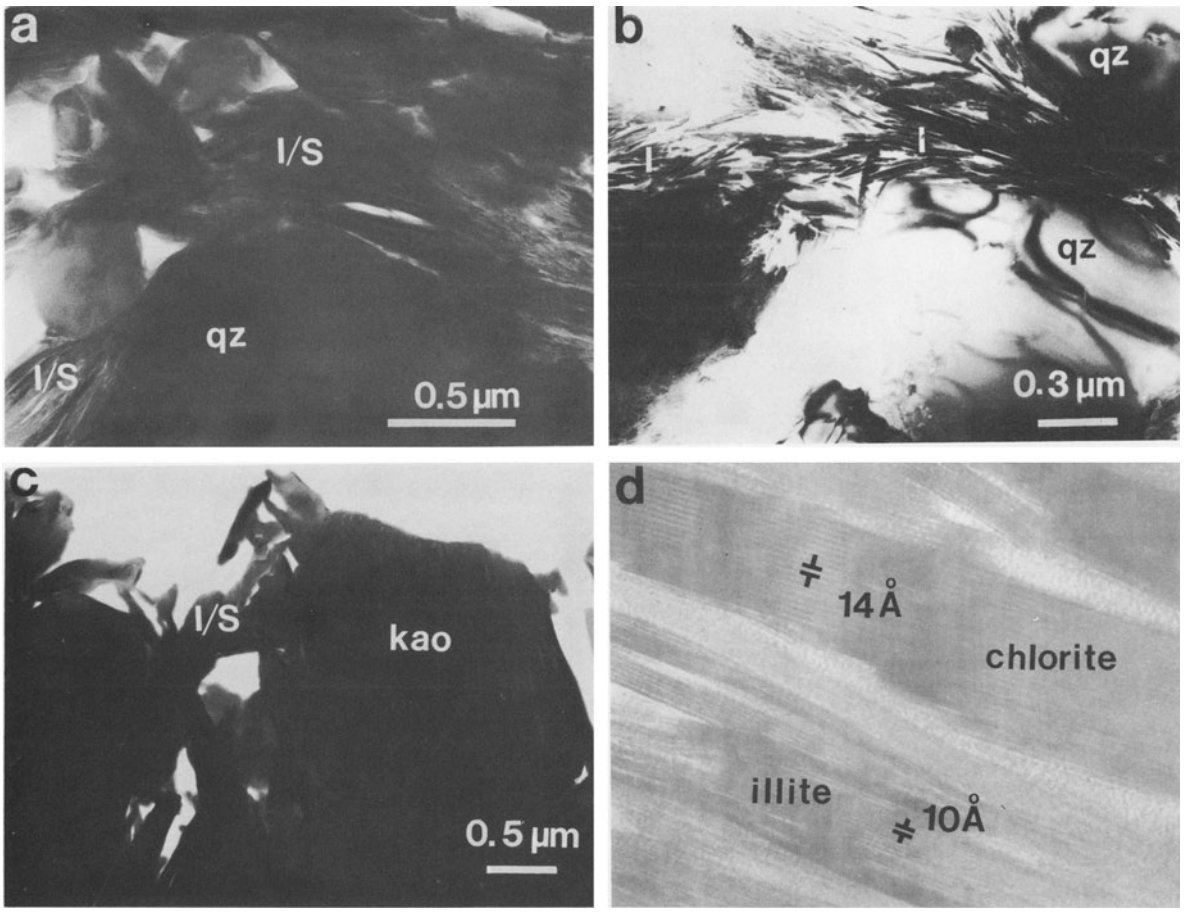

Figure 2. (a) Transmission electron microscopic image showing the typical clay mineral texture in shales found at shallow depth (384 m, 170°C). Clay minerals, mostly interstratified illite/smectite (I/S) occur as anastomosing units wrapped around non-phyllosilicates. (b) Discrete illite (I) crystals tangentially filling interstitial pore space (256 m, 115°C). (c) Large detrital grain of kaolinite found at 256 m depth (115°C). (d) Diagenetic chlorite found within a matrix of I/S layers (384 m, 170°C).

MINERALOGY AND MINERAL CHEMISTRY

The mineral assemblages at different depths and temperatures are shown in Figure 1. On the basis of the first appearance of each of the phases, three phyllosilicate zones can be identified: illite (115°–220°C), chlorite (220°–310°C), and biotite (>310°C). Textures, modes of occurrence, and compositions of minerals in each zone are described below.

Illite zone

Illite from this zone was described in detail by Yau *et al.* (1987a) and is therefore only briefly described here. At shallow depths (<549 m) illite occurs in three modes: (1) as packets of layers interstratified with smectite (I/S), (2) as discrete crystals in pore space, and (3) as detrital grains having diameters of a few micrometers. The detrital illite is not considered in the following descriptions.

I/S typically forms continuous anastomosing units wrapped around detrital grains of non-phyllosilicates (Figure 2a). Its texture is similar to that observed for I/S in Gulf Coast shales (Ahn and Peacor, 1986). The borders of I/S are irregular. The amount of illite relative to smectite in I/S increases, but the total of I/S decreases with increasing depth, as determined by XRD (Yau *et al.*, 1987a). I/S was not detected by XRD or TEM in samples from depths >540 m (220°C).

Discrete illite crystals were observed in pore space in samples from a depth of 256 m (115°C) (Figure 2b). Because samples shallower than this depth were not available, such discrete illite crystals may occur at even lower temperatures. The illite forms subhedral to euhedral, pseudohexagonal plates a few micrometers wide and about 300 Å thick. It increases in abundance with increasing depth to 732 m (260°C), but rapidly decreases in abundance below that depth. Its well-defined crystal outlines and occurrence in pore spaces suggest

https://doi.org/10.1346/CCMN.1988.0360101 Published online by Cambridge University Press

Table 1. Averaged analytical electron microscopic analyses for authigenic phyllosilicates in well IID2, Salton Sea geothermal field.[1]

	Illite			Chlorite		Biotite	
Depth (m)	256	540	732	983	1259	1259	1547
Temp. (°C)	115	220	260	300	310	310	330
No. of analyses	18	19	26	15	13	9	24
Si	3.3 (0.2)[4]	3.3 (0.2)	3.4 (0.2)	3.2 (0.2)	3.2 (0.3)	3.2 (0.2)	3.1 (0.2)
Al^{IV}	0.7	0.7	0.6	0.8	0.8	0.8	0.9
Al^{VI}	1.5 (0.1)	1.5 (0.2)	1.5 (0.2)	0.9 (0.2)	1.3 (0.4)	0.0 (0.1)	0.3 (0.2)
Mg	0.3 (0.1)	0.2 (0.1)	0.2 (0.1)	3.1 (0.3)	2.1 (0.4)	1.6 (0.1)	1.6 (0.2)
Fe^2	0.2 (0.1)	0.3 (0.2)	0.3 (0.1)	2.0 (0.2)	2.6 (0.3)	1.4 (0.1)	1.1 (0.2)
K	0.7 (0.2)	0.7 (0.2)	0.8 (0.1)	0.0 (0.1)	0.0 (0.1)	1.0 (0.1)	1.0 (0.2)
OH^3	1.7	1.8	2.0	7.9	7.5	1.9	1.5
O^3	10.0	10.0	10.0	10.1	10.4	10.2	10.5

[1] Normalized to Σ cations − K = 6 for illite, 7 for biotite and Σ cations = 10 for chlorite.
[2] Fe = Fe^{3+} for illite, Fe = Fe^{2+} for chlorite and biotite.
[3] OH/O calculated for charge balance.
[4] One standard deviation given in parentheses.

that such illite is authigenic and that it crystallized directly from solution. These discrete illite crystals have significant amounts of Mg and Fe substituting for octahedral Al (Table 1). The interlayer K ranges from 0.7 to 0.8 moles per formula unit and shows little variation with depth. The relatively uniform size and shape of all SSGF illites at all depths, coupled with a lack of compositional zoning within individual illites, imply that early-formed crystals underwent no further reaction with increasing depth.

Kaolinite occurs as discrete grains a few micrometers thick (Figure 2c). The relatively large grain size and irregular outline of the kaolinite suggest that it is detrital. Qualitative AEM analyses of large kaolinite grains show the presence only of Al and Si, and the electron diffraction patterns show only a 7-Å 001 spacing. These features suggest that no other phyllosilicate is intergrown with or replaces the kaolinite. Chlorite in this zone occurs locally as packets of layers within I/S (Figure 2d) in a manner similar to that in Gulf Coast shales (Ahn and Peacor, 1985). The 001 lattice-fringe images of some of the packets of chlorite layers showed 7-Å serpentine-like layers (berthierine) in addition to 14-Å fringes. The former has been found intercalated with 14-Å chlorite in Gulf Coast shales from shallow depths, but not in deep samples (Ahn and Peacor, 1985). Ahn and Peacor (1985) inferred that the 7-Å serpentine-like structure is a low-temperature, metastable polymorph of a 14-Å chlorite and that it was derived along with coexisting illite as a reaction product of smectite.

Chlorite zone

Individual crystals of chlorite were first encountered at a depth of 540 m (220°C) as euhedral to subhedral crystals and coexisting with illite crystals in pore spaces (Figure 3a). Both the chlorite and illite have well-defined crystal shapes, and no direct layer-to-layer transformation between them was observed. These features suggest that the illite and chlorite in this zone crystallized simultaneously from solution. Detrital I/S present in the original sediments was not found coexisting with discrete illite and chlorite in this zone. Kaolinite, dolomite, and ankerite, present in shallow samples, are conspicuously absent in the chlorite zone. The chlorite content increases with depth, and chlorite is the dominant phyllosilicate in the interval of 983–1360 m. Illite is rare in this interval, but where present, it is euhedral. The chlorite occurs principally as individual, euhedral grains in open pore space (Figure 3b), consistent with a growth mechanism of direct crystallization from solution. The (001) lattice-fringe images of chlorite (Figure 3c) display only 14-Å layer spacings and no 7-Å serpentine-like layers. The fringes are usually straight and free of dislocations. Only at the contacts between grains were layer terminations observed, mainly as periodic arrays typical of low-angle grain boundaries (Figure 3c). Deformation features such as kink banding (Figure 3d) were observed in chlorite, presumably the result of compaction during grain growth.

Averaged analyses of chlorite (Table 1) show that the amount of octahedral Al is greater than tetrahedral Al. The resulting excess positive charge may be compensated by the substitution of oxygen in the hydroxyl site. The composition of chlorite within a sample is similar, while the composition of chlorite at different depths is significantly different. Chlorite found at greater depths has a higher Fe content (Fe/(Fe + Mg) = 0.6) than that from shallower depths (Fe/(Fe + Mg) = 0.4). The amounts of albite and K-feldspar increase in the deeper parts of the chlorite zone (>900 m).

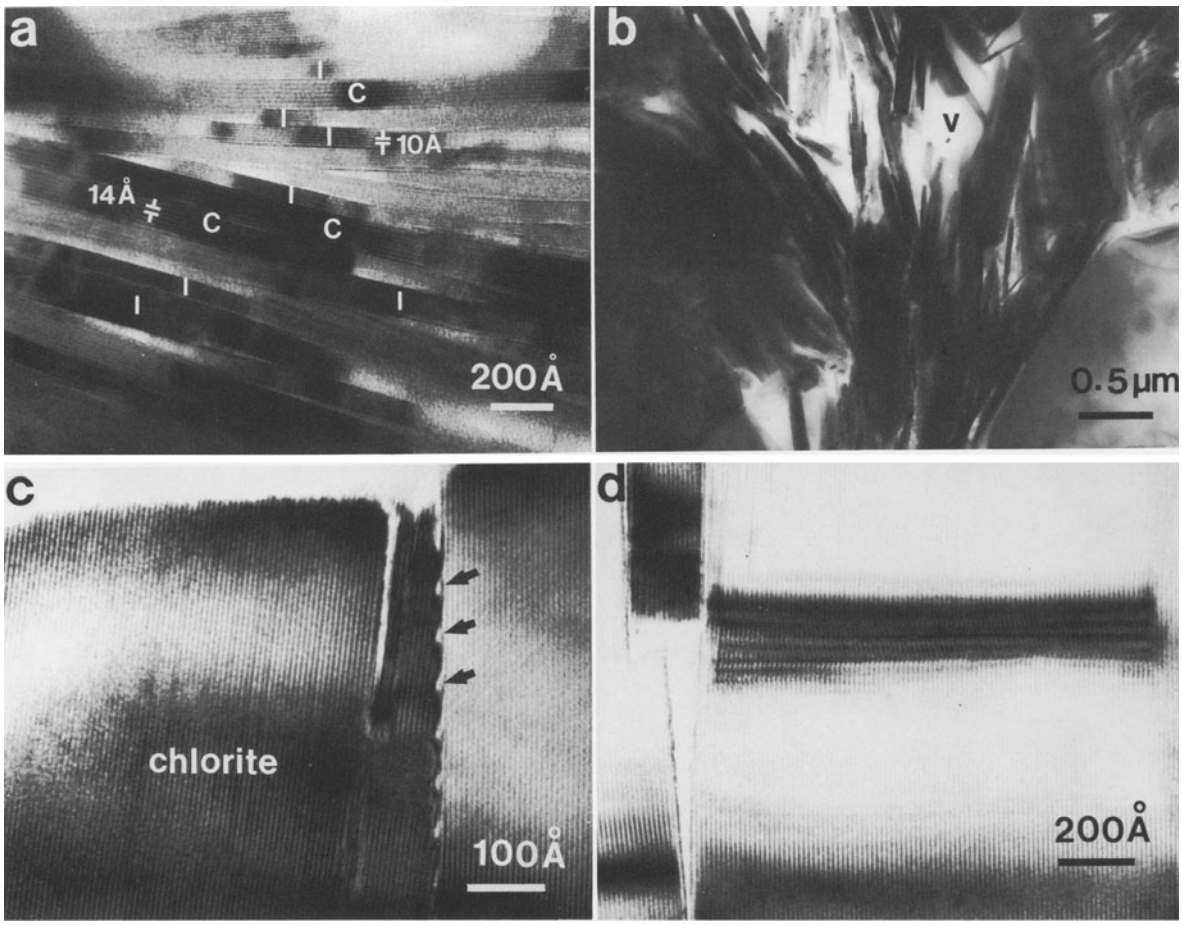

Figure 3. (a) Lattice-fringe images of individual crystals of illite (I) and chlorite (C) in the chlorite zone (732 m, 260°C). (b) Authigenic chlorites formed as discrete, euhedral to subhedral crystals filling interstitial pore spaces (983 m, 330°C). Void space (v) was filled with casting resin during sample preparation. (c) Lattice-fringe images of chlorites (983 m, 300°C) showing layer terminations at one end of a crystal (upper line) and edge dislocations along grain boundary (arrows). (d) Kink banding in chlorite crystal as result of compaction during grain growth (983 m, 300°C).

Biotite zone

Biotite was first found at a depth of 1259 m (310°C) as rare, discrete, euhedral grains coexisting with chlorite and filling pore spaces (Figure 4a). Biotite is more abundant with increasing depth, to a depth of 1547 m (330°C). Chlorite is subordinate in the 1259–1547-m depth interval, but still shows euhedral outlines, implying that it has not undergone dissolution. Biotite commonly coexists with K-feldspar (Figure 4b). The K-feldspar and albite contents remain high throughout most of the biotite zone, although the proportion of albite is smaller in the deepest sample investigated (1547 m). The composition of K-feldspar is nearly pure end-member $KAlSi_3O_8$, and the grains contain no exsolution lamellae, consistent with an authigenic origin. The biotite commonly displays growth steps (Figure 4c) which suggest direct crystallization from solution by growth by addition of layers. The (001) lattice-fringe images of biotite show continuous, straight layers having characteristic 10-Å layer spacings (Figure 4d). Imperfections, such as edge dislocations and low-angle grain boundary-like features are common, but mixed-layering with other phyllosilicates was not observed. The growth steps and euhedral character of biotite grains projecting into pore space provide strong evidence for an origin through direct crystallization from solution. Biotite rarely occurs as packets of layers intergrown with packets of chlorite layers.

Averaged, normalized biotite analyses yield the atomic ratio $Fe/(Mg + Fe + Al^{VI}) = 0.4–0.5$ (Table 1). The formulae have a higher Fe content than those of biotite (0.2) formed at an equivalent temperature (330°C) in sandstone (McDowell and Elders, 1980). In addition, the analyses given here are consistent with full occupancy of K in the interlayer sites, whereas the

https://doi.org/10.1346/CCMN.1988.0360101 Published online by Cambridge University Press

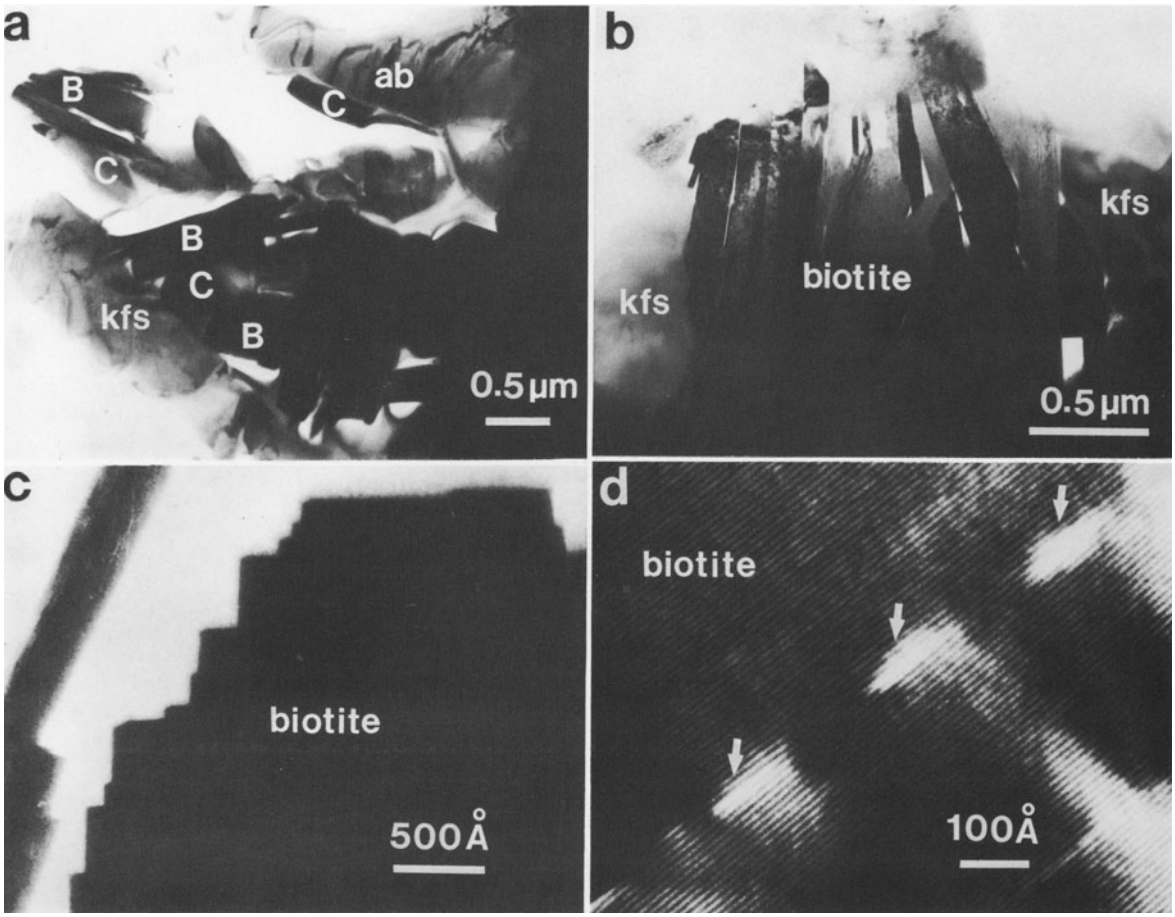

Figure 4. (a) Transmission electron microscopic image showing discrete chlorite (C) and biotite (B) crystals at 1360 m depth (320°C). (b) Intergrown authigenic biotite and authigenic K-feldspar from 1515 m depth (320°C). (c) Growth steps on biotite crystal found within pore space, indicating direct crystallization from solution, with growth by addition of layers. (d) Lattice-fringe images of biotite (1515 m, 320°C) showing abundant edge dislocations (arrows) regularly spaced along a low-angle grain boundary.

analyses of biotite from sandstones suggest a high proportion of vacancies in large cation sites (~40%). The Salton Sea biotite has a relatively low Al content relative to biotite from low-grade pelitic rocks (Ferry, 1985).

WHOLE-ROCK CHEMISTRY

The weight percentages of major, non-volatile components of shale cuttings from selected depths (Table 2) show that Na, K, and Ca vary significantly with

Table 2. X-ray fluorescence analyses of shales from well IID No. 2, Salton Sea geothermal field.

Zone	Illite		Chlorite		Biotite		
Depth (m)	384	476	983	1079	1320	1384	1534
Temp. (°C)	160	190	300	306	320	322	328
SiO_2	54.50	55.10	56.20	54.40	56.70	56.40	56.00
TiO_2	0.72	0.68	0.72	0.69	0.66	0.67	0.67
Al_2O_3	19.00	17.80	15.50	15.40	17.20	17.00	17.10
Fe_2O_3	5.58	5.67	5.68	6.55	4.38	4.64	6.55
MgO	3.38	3.70	4.54	5.00	4.18	3.19	3.42
CaO	4.39	5.62	5.17	4.23	4.98	2.49	1.92
Na_2O	0.60	0.53	2.85	2.67	2.16	2.68	1.55
K_2O	3.82	3.95	3.37	4.13	5.62	7.45	9.08
P_2O_5	0.13	0.14	0.15	0.15	0.15	0.13	0.12
Total	92.08	93.19	94.17	93.26	96.02	95.41	96.40

https://doi.org/10.1346/CCMN.1988.0360101 Published online by Cambridge University Press

depth, but that the variation of other major elements with depth is small. The variations in rock chemistry with depth correspond to changes in mineral assemblages. Thus, from the illite through the chlorite to the biotite zone, the shales show a decrease in CaO as the calcite content decreases, an increase in Na with increased albite, and an increase in K with increased K-feldspar and biotite. Evidence presented by Muffler and Doe (1968) indicates that sediments deposited in the Salton Sea trough were of similar chemical and mineralogical composition throughout the sequence studied. The variations in whole-rock chemistry with depth must therefore be the result of post-burial hydrothermal activity, suggesting that the shales have acted as open systems with the introduction and loss of elements during diagenesis.

DISCUSSION

The presence of pore spaces separating individual, euhedral to subhedral grains of illite, chlorite, and biotite indicates that these phyllosilicates formed through nucleation and crystal growth from pervasive aqueous solutions rather than by direct replacement of pre-existing phases. Thus, reaction mechanisms in the Salton Sea argillaceous sediments principally involve dissolution of original phases, transportation of dissolved species by convecting fluid, and crystallization from solution. The coarse-grained sandstones in the SSGF display similar zones of phyllosilicates over similar temperature-depth intervals (Muffler and White, 1969; McDowell and Elders, 1980) as observed in the shales studied here. Based on the regularity of mineralogy in the SSGF, Zen and Thompson (1974) inferred that the rocks responded systematically to the physiochemical environment and approached equilibrium. Our observations on the fine-grained rocks support their conclusion. In addition, mixed-layering of more than one phase, which commonly occurs in diagenetic and low-grade metamorphic phyllosilicates and which represents a non-equilibrium state for such phases (Lee *et al.*, 1984, 1985), is *not* common in Salton Sea phyllosilicates. Similarly, the phyllosilicate crystals are free of pervasive imperfections such as layer terminations that characterize phyllosilicates in the Gulf Coast shales (Lee *et al.*, 1985; Ahn and Peacor, 1986). These features are consistent with the assumption that the diagenetic mineral assemblages and the interstitial fluids approached equilibrium relative to the original detrital suites. Such relations permit identification of product and reactant phases, especially by comparison with the obvious non-equilibrium textural features displayed by detrital minerals at shallow depths.

Fluid-mineral equilibria

Activity-activity equilibrium diagrams that represent first approximations of phyllosilicate stability relations under various thermal and fluid-composition conditions were calculated using the mineral compositional data obtained in this study. Equations used for mineral–mineral equilibria in the system K_2O-MgO-Al_2O_3-SiO_2-H_2O-H^+ and hydrolysis constants for end-member solid phases, except for clinochlore, are taken from Bowers *et al.* (1984). Activities of phases appearing as components in solid solutions in the drill cuttings studied were calculated as given in Table 3. Figure 5 depicts the results of calculations of stability relations among K-feldspar, phlogopite (biotite), muscovite (illite), clinochlore (chlorite), and kaolinite in terms of the ion activity ratios $(K^+)/(H^+)$ and $(Mg^{2+})/(H^+)^2$ in a coexisting aqueous solution in equilibrium with quartz. The numerical coordinates of the axes calculated at 300°C apply only to the K-feldspar-biotite, K-feldspar-illite, and illite-kaolinite boundaries.

The chlorite stability field in Figure 5 is drawn schematically to agree with the mineral compatibilities observed in this study. If the hydrolysis constants for clinochlore given by Bowers *et al.* (1984) and the mineral compositions determined in this study are used, the assemblage biotite + illite is stable relative to chlorite + K-feldspar over a temperature range that includes the 250°–330°C increment covered by this study. The mineral associations indicate that biotite + illite is unstable with respect to, and is replaced by, chlorite + K-feldspar near the first appearance of biotite. Because coexisting chlorite and K-feldspar grains are euhedral, their coexistence suggests that they are in equilibrium. Moreover, chlorite + K-feldspar is a common hydrothermal mineral assemblage at temperatures of 350°C or lower in both experimental and natural systems (Hoschek, 1973; Beane and Titley, 1981). The discrepancy between the calculated relations and the observed assemblages may be due to the thermodynamic properties of the chlorite, which are still not well understood.

The phase relations shown in Figure 5 can be interpreted in two ways to account for the mineralogical zonation with depth seen in the drill hole. The first relates to an increase in temperature with depth, whereas the second involves changing activities of ions in an ascending fluid.

Significance of temperature effects

As temperature increases, stability fields of the pure phases move to progressively lower $(K^+)/(H^+)$ and $(Mg^{2+})/(H^+)^2$ ratios (shown by the arrow in Figure 5; cf. Hemley *et al.*, 1971; Montoya and Hemley, 1975; Bowers *et al.*, 1984). Therefore, the apparent increase in cation activity ratios with increasing depth in the drill hole, as indicated by successive mineral assemblages (i.e., point E to point B successively, Figure 5), is compatible with the collapse of the mineral stability fields toward the origin with increasing temperature for constant ionic activity ratios in the solution. Fixed ion-activity ratios do not, however, necessarily correspond

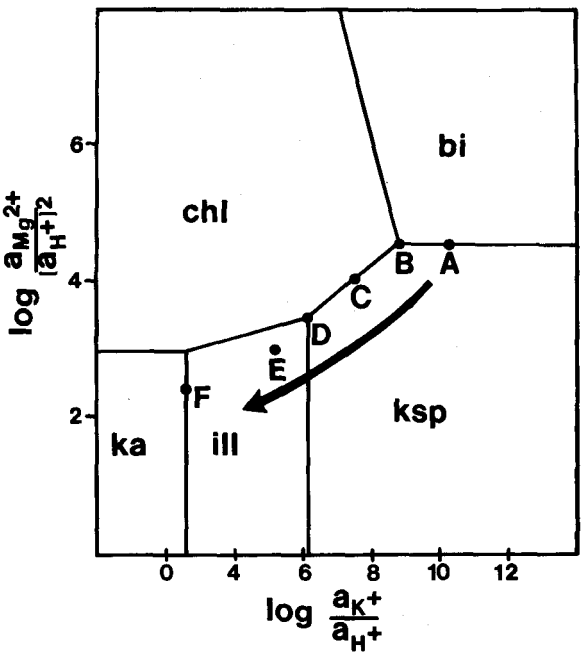

Figure 5. Mineral stability diagram showing calculated phase relations among K-feldspar, biotite, clinochlore, muscovite, and kaolinite in terms of the composition of a coexisting aqueous phase in equilibrium with quartz at 300°C. The K-feldspar-biotite, K-feldspar-illite, and illite-kaolinite boundaries are drawn using hydrolysis constants given by Bowers *et al.* (1984). Chlorite stability field is schematically drawn to correspond to phase relations observed in the drill hole. Arrow indicates the direction of stability field movement with increasing temperature.

to fixed concentration ratios in an aqueous solution. The Salton Sea geothermal fluid, which can be considered responsible for the hydrothermal mineral assemblages described here, is a highly concentrated chloride brine with an equivalent NaCl concentration of nearly 6 molal (Helgeson, 1968). It is not currently possible to convert from total concentration of various cations to their corresponding individual ion activities, or vice versa, due to the unknown effects of individual ion-activity coeffcients and ion association reactions in brines of such high chloride concentrations at elevated temperatures. Furthermore, individual ion-activity coefficients and degrees of ion association vary as a function of temperature (cf. Helgeson, 1969). For example, the total-concentration ratio of KCl/HCl in a fluid coexisting with muscovite, K-feldspar, and quartz decreases at a faster rate with increasing temperature than does the corresponding calculated $(K^+)/(H^+)$ ion-activity ratio (Montoya and Hemley, 1975). Thus, the position of a fixed aqueous solution composition on Figure 5 is likely to change with temperature as do the mineral stability relations. Although it is possible that the mineral depth-zoning might be caused by the effects

Table 3. Activities of phases used to calculate Figure 5.

Muscovite	$a = X_K(X_{Al,O})^2(X_{OH})^2$
Phlogopite	$a = X_K(X_{Mg,O})^3(X_{OH})^2$
Clinochlore	$a = (X_{Mg,O})^5(X_{Al,O})(X_{OH})^8/(5/6)^5(1/6)$
Kaolinite	$a = 1$
K-feldspar	$a = 1$
Water	$a = 0.9$ (Helgeson, 1967)

of increasing temperature in the drill hole on a system containing a hydrothermal fluid of constant composition, a quantitative evaluation of the solution-mineral equilibria cannot be carried out at the present time.

Significance of variation in ion concentration with depth

A second mechanism which may control mineral zoning involves irreversible reaction between the geothermal brine and original detrital minerals with which the aqueous solution is not in equilibrium. If a solution initially in equilibrium with biotite and K-feldspar (point A in Figure 5) were to react with kaolinite, first biotite, then chlorite, and finally illite would be produced as intermediate reaction products (cf. Helgeson, 1970; Helgeson *et al.*, 1969). If the fluid was ascending as the overall reaction proceeded, these minerals would be zoned progressively upward with depth, as observed. The reaction path might progressively follow the points B, C, D, E, and F (Figure 5) corresponding to decreasing cation activity ratios, due chiefly to generation of hydrogen ion in the brine by reactions such as:

$$Al_2Si_2O_5(OH)_4 + 2\,K^+ + 6\,Mg^{2+} + 4\,SiO_2 + 7\,H_2O = 2\,KMg_3AlSi_3O_{10}(OH)_2 + 14\,H^+.$$

Such a simplified process of irreversible reactions would, of course, be complicated by the effects of decreasing temperature on mineral stabilities and brine chemistry as discussed above.

Although either increase in temperature or changing ion concentrations with depth are capable of explaining the observed mineral zoning, the relative effect of each variable cannot now be assessed. Determination of the significance of each depends on the availability of additional data, including ion concentrations as a function of depth and definition of the fluid-flow regime, both in terms of the volume and flow direction for a given mineral-depth sequence.

Reaction progress vs. time

The minerals may have altered during a short-lived episodic hydrothermal event or over a longer time interval, similar to that for burial metamorphism. In an episodic event, a hydrothermal brine or heat source would have been introduced rapidly into the sediments giving rise to an elevated thermal gradient and/or al-

https://doi.org/10.1346/CCMN.1988.0360101 Published online by Cambridge University Press

tered fluid chemistry in a short time interval. Smectite would react to form authigenic illite at shallow depths and low temperatures, and might also react directly to form chlorite or biotite at greater depths (temperatures) without producing intermediate phases. This mechanism requires that reaction rates were slow relative to the rate of increase of temperature, and that reactions would cease once products and fluids equilibrated. The uniform size and homogeneity of composition of authigenic phyllosilicate crystals at all depths are compatible with such an episodic process. Although the sediments are of Pliocene to Pleistocene age, the Salton Sea geothermal field is estimated to have been active for only 16,000 years (Kistler and Obradovich, in Muffler and White, 1969). Such a short time period relative to the age of sedimentation is consistent with an episodic hypothesis.

In burial metamorphism, detrital sediments as well as the earlier-formed minerals would pass through a continuous sequence of transformations with increasing time. Consequently, the hydrothermal alteration over a long time interval would result in a series of replacement reactions, i.e., chlorite by biotite and illite by chlorite, or dissolution of pre-existing phases. The absence of such textures raises the question as to whether or not sequential changes in the same layer took place with increasing burial depth. Indeed, Morton (1985a, 1985b) hypothesized on the basis of isotope data that the diagenetic reactions in the Gulf Coast sequence represent a single event rather than a series of continuous changes with increasing burial.

If the alteration process indeed occurred by changing the original mineral phases directly to form chlorite or biotite at greater depths over a short time period, the following series of irreversible reactions may be formulated, two of which utilize the muscovite component of illite/smectite:

$$\text{muscovite} + 5\ \text{dolomite} + 3\ \text{quartz} + 3\,H_2O = \text{chlorite} + \text{K-feldspar} + 5\ \text{calcite} + 5\,CO_2. \quad (1)$$

$$5\ \text{dolomite} + \text{kaolinite} + \text{quartz} + 2\,H_2O = \text{chlorite} + 5\ \text{calcite} + 5\,CO_2. \quad (2)$$

$$5\ \text{muscovite} + 12\ \text{dolomite} + 4\ \text{kaolinite} + 10\ \text{quartz} = 4\ \text{phlogopite} + 6\ \text{clinozoisite} + \text{K-feldspar} + 6\,H_2O + 24\,CO_2. \quad (3)$$

Reaction (2) was suggested by Zen (1959) as an isograd for the coexistence of calcite and chlorite in many low-grade metamorphic rocks, whereas reactions (1) and (3) are described here for the first time. These reactions involve metastable mineral assemblages as reactants, however, and do not represent equilibrium phase relations as normally denoted by univariant phase equilibria. They may be taken as an indication of the relative reactivity of various detrital assemblages rather than representing closed system behavior as in ordinary metamorphism.

Phase equilibria for these reactions can be calculated at the measured in-hole pressure of 0.1 kbar for ideal mixing of CO_2 and H_2O using the program THERMO (Perkins *et al.*, 1987). Results of the calculations suggest that the temperature for chlorite formation is lower than that for biotite formation, consistent with temperature as a factor controlling the depth-zoning of phyllosilicates, as suggested above. The calculations, however, yield qualitative results at present due to the unknown corrections for non-ideality of CO_2 and H_2O mixing at low temperatures and pressures (Yau *et al.*, 1987b), and of the effects of solid solutions in minerals.

Although the textural, chemical and structural relations observed in this study are all compatible with results of an episodic hydrothermal alteration in an open system, it must remain as a tentative hypothesis subject to the definition of many other kinds of data, especially as relate to the flow regime and solution chemistry as a function of depth. Current drilling in the Salton Sea area may well provide such data (Elders, 1984).

ACKNOWLEDGMENTS

We are grateful to B. H. Wilkinson for critical review of the manuscript and to W. C. Bigelow for maintaining the University of Michigan Electron Microbeam Analysis Laboratory. This work was supported by NSF grants EAR-8107529 and EAR-8313236 to D. R. Peacor. The STEM used in this study was acquired under the Grant No. DMR-77-09643, the SEM under BSR-83-14092, and the EMPA under EAR-8212764 from NSF.

REFERENCES

Ahn, J. H. and Peacor, D. R. (1985) Transmission electron microscopic study of diagenetic chlorite in Gulf Coast argillaceous sediments: *Clays & Clay Minerals* **33,** 228–237.

Ahn, J. H. and Peacor, D. R. (1986) A transmission and analytical electron microscopic study of the smectite to illite transition: *Clays & Clay Minerals* **34,** 165–180.

Beane, R. E. and Titley, S. R. (1981) Porphyry copper deposits. Part II. Hydrothermal alteration and mineralization: *Econ. Geol.* **75,** 238–269.

Bird, D. K. and Norton, D. L. (1981) Theoretical predictions of phase relations among aqueous solution and minerals: Salton Sea geothermal system: *Geochim. Cosmochim. Acta* **45,** 1479–1493.

Bird, D. K., Schiffman, P., Elders, W. A., Williams, A. E., and McDowell, S. C. (1984) Calc-silicate mineralization in active geothermal systems: *Econ. Geol.* **79,** 671–695.

Bowers, T. S., Jackson, K. J., and Helgeson, H. C. (1984) *Equilibrium Activity Diagrams for Coexisting Minerals and Aqueous Solutions at Pressures and Temperatures to 5 Kbar and 600°C:* Springer-Verlag, New York, 397 pp.

Burst, J. F. (1969) Diagenesis of Gulf Coast clay sediments and its possible relation to petroleum migration: *Amer. Assoc. Petroleum Geol. Bull.* **53,** 73–93.

Elders, W. A. (1984) *Proposed Scientific Activities for the*

Salton Sea Scientific Drill Projects: Earth Sciences Division, Lawrence Berkeley Laboratory (LBL-17717), 132 pp.

Ferry, J. M. (1985) A biotite isograd in south-central Maine, U.S.A.: Mineral reactions, fluid transfer, and heat transfer: *J. Petrol.* **25,** 871–893.

Helgeson, H. C. (1967) Solution chemistry and metamorphism: *Researches in Geochemistry, Vol. 2,* P. H. Abelson, ed., Wiley, New York, 362–402.

Helgeson, H. C. (1968) Geologic and thermodynamic characteristics of the Salton Sea Geothermal System: *Amer. J. Sci.* **266,** 129–166.

Helgeson, H. C. (1969) Thermodynamics of hydrothermal systems at elevated temperatures and pressures: *Amer. J. Sci.* **267,** 729–804.

Helgeson, H. C. (1970) A chemical and thermodynamic model for ore deposition in hydrothermal systems: *Mineral. Soc. Amer. Special Paper* **3,** 155–186.

Helgeson, H. C., Garrels, R. M., and Mackenzie, F. T. (1969) Evaluation of irreversible reactions in geochemical processes involving minerals and aqueous solutions: II. Applications: *Geochim. Cosmochim. Acta* **32,** 455–482.

Hemley, J. J., Montoya, J. W., Nigini, A., and Vincent, H. A. (1971) Some alteration reactions in the system CaO-Al_2O_3-SiO_2-H_2O: *Soc. Mining Geol. Japan Spec. Issue* **2,** 58–63.

Hoschek, G. (1973) Zur Stabilitat metamorpher biotit-paragenesen: *Tschermaks Mineral. Petrol. Mitt.* **20,** 48–58.

Hower, J., Eslinger, E. V., Hower, M. E., and Perry, E. A. (1976) Mechanism of burial metamorphism of argillaceous sediments: 1. Mineralogical and chemical evidence: *Geol. Soc. Amer. Bull.* **87,** 725–737.

Isaacs, D., Brown, P. E., Valley, J. W., Essene, E. J., and Peacor, D. R. (1981) An analytical study of a pyroxene-amphibole intergrowth: *Contrib. Mineral. Petrol.* **77,** 115–120.

Lee, J. H., Peacor, D. R., Lewis, D. D., and Wintsch, R. P. (1984) Chlorite-illite/muscovite interlayered and interstratified crystals: A TEM/AEM study: *Contrib. Mineral. Petrol.* **88,** 372–385.

Lee, J. H., Ahn, J. H., and Peacor, D. R. (1985) Textures in layer silicates: Progressive changes through diagenesis and low temperature metamorphism: *J. Sed. Petrol.* **55,** 532–540.

Maxwell, D. T. and Hower, J. (1967) High-grade diagenesis and low-grade metamorphism of illite in the Precambrian Belt Series: *Amer. Mineral.* **52,** 843–857.

McDowell, S. D. and Elders, W. A. (1980) Authigenic layer silicate minerals in borehole Elmore 1, Salton Sea geothermal field, California, U.S.A.: *Contrib. Mineral. Petrol.* **74,** 293–310.

McDowell, S. D. and Elders, W. A. (1983) Allogenic layer silicate minerals in borehole Elmore #1, Salton Sea geothermal field, California: *Amer. Mineral.* **68,** 1146–1159.

Montoya, J. W. and Hemley, J. J. (1975) Activity relations and stability in alkalic feldspar and mica alteration reactions: *Econ. Geol.* **70,** 577–583.

Morton, J. P. (1985a) Rb-Sr evidence for punctuated illite/smectite diagenesis in the Oligocene Frio Formation, Texas Gulf Coast: *Geol. Soc. Amer. Bull.* **96,** 114–122.

Morton, J. P. (1985b) Rb-Sr dating of diagenesis and source age of clays in Upper Devonian black shales of Texas: *Geol. Soc. Amer. Bull.* **96,** 1043–1049.

Muffler, L. P. J. and Doe, B. R. (1968) Composition and mean age of detritus of the Colorado River delta in the Salton trough, southeastern California: *J. Sed. Petrol.* **38,** 384–399.

Muffler, L. P. J. and White, D. E. (1969) Active metamorphism of Upper Cenozoic sediments in the Salton Sea geothermal field and the Salton trough, southeastern California: *Geol. Soc. Amer. Bull.* **80,** 157–182.

Perkins, D., Essene, E. J., and Wall, V. J. (1987) THERMO: A computer program for calculation of mixed volatile equilibria: *Amer. Mineral.* **72,** 446–447.

Perry, E. and Hower, J. (1970) Burial diagenesis in Gulf Coast pelitic sediments: *Clays & Clay Minerals* **18,** 165–177.

Robinson, P. T., Elders, W. A., and Muffler, L. P. J. (1976) Quaternary volcanism in the Salton Sea geothermal field, Imperial Valley, California: *Geol. Soc. Amer. Bull.* **87,** 347–360.

Velde, B. and Hower, J. (1963) Petrological significance of illite polymorphism in Paleozoic rocks: *Amer. Mineral.* **48,** 1239–1254.

Weaver, C. E. (1959) The clay petrology of sediments: in *Clays and Clay Minerals, Proc. 6th Natl. Conf., Berkeley, California, 1957,* Ada Swineford, ed., Pergamon Press, New York, 154–187.

Yau, Y. C., Peacor, D. R., and McDowell, S. D. (1987a) Smectite-illite reactions in Salton Sea shales: *J. Sed. Petrol.* **57,** 335–342.

Yau, Y. C., Peacor, D. R., and Essene, E. J. (1987b) Authigenic anatase and titanite in shales from the Salton Sea geothermal field, California: *Neues Jahr. Mineral. Monat.* **10,** 441–452.

Zen, E-an (1959) Clay mineral-carbonate relations in sedimentary rocks: *Amer. J. Sci.* **257,** 29–43.

Zen, E-an and Thompson, A. B. (1974) Low grade regional metamorphism: Mineral equilibrium relations: *Annual Rev. Earth Planetary Sci.* **2,** 179–212.

(Received 21 February 1987; accepted 27 July 1987; Ms. 1649)